## Solar PV Potential and Energy Demand Assessment in Machakos County

K. Muchiri[1*], J. N. Kamau[2], D. W. Wekesa[3], C. O. Saoke[4], J. N. Mutuku[5], J. K. Gathua[6]

[1*, 2, 4, 5] Department of Physics, Jomo Kenyatta University of Agriculture and Technology, Kenya

[3]Department of Physics, Machakos University, Kenya

[6] Department of Physics, Kenyatta University, Kenya.

**Abstract**

Machakos County has the need for renewable energy access due to its rapid industrial development, growing population, higher living standards and rural electrification. Wind-solar hybrid off-grid system has therefore been proposed for small scale energy production suitable for Machakos County rural areas. This paper presents the solar photovoltaic (PV) potential assessment results and a survey done to investigate the levels of energy use, and economic potential of the energy consumers in three rural zones adjacent to Machakos town. Assessment of solar PV potential was done using the Photovoltaic Geographical Information System (PVGIS), a tool that gives access to PV performance and solar radiation patterns for a period of over 10 years. Monthly variations in energy output and solar irradiation were investigated at a fixed angle of Inclination of $10^o$, Azimuth angle of $-180^o$ , latitude and longitude of $1.531\,^oS$ $37.262\,^oE$, and an altitude of 1623 m above sea level. Measured values of Global Horizontal Irradiance from the site using MS-602 pyranometer were used for comparison. Yearly average PV energy production and yearly in-plane irradiation were determined as 1740 kWh and 2130 kWh/$m^2$ at an installed capacity of 1kWp. This yearly average energy value was used in sizing of the solar panels and battery capacities required for the wind- solar hybrid system installation. The End-use method was used to determine the energy utilization levels in the rural homes where a questionnaire with a sample of 100 households per zone was used for data collection. The questionnaire items included household income, average month electricity bill, power rating of appliance used, house hold size and daily use time of each electrical appliance collected via end-use method. The energy load demand was 782.7 kWh, 841.2 kWh and 620.02 kWh per day for zones A, B and C respectively. Demand per household differed depending on household size and the appliances present. The household's peak energy consumption was 9.09 kWh and a minimum of 0.052 kWh per day. The average energy demand per household was 2.429 kWh, 2.26 kWh and 2.347 kWh in the three zones respectively. Monthly income and daily load demand profiles were plotted to investigate the energy use patterns and the economic status of the energy consumers in the three zones.

**Key words:** Solar PV Potential, PVGIS, Energy Load Demand, Wind-Solar Hybrid, Renewable Energy, Rural Electricity Consumption, Machakos county rural energy load

## INTRODUCTION

### Solar PV

The world level of energy consumption is rapidly increasing creating a high demand for energy. This exponential rise in energy demand attributed to the growing population, urbanization and industrial developments, rural electrification and the rise in people's living standards [1]. With the country's vision of industrialization by the year 2030, new approaches to energy generation are paramount. In Kenya, energy is mainly from electricity (9%), petroleum fuels (22%) and biomass (68%) [2]. In the rural areas, most of the conventional sources of energy used highly impact negatively to the environment and life due to the hazardous emissions that lead to pollution and global warming [3], [4], [5], [6], [7], [8]. This trend can be reversed by diversifying ways of energy sourcing, attracting the use of inexhaustible and friendlier renewable energy sources [9]. Modern sustainable technologies of energy harvesting from renewable sources like wind and solar need to be embraced to support and enhance energy self-sufficiency in both urban and rural areas [2]. To help in renewable energy development in rural areas, a wind-solar hybrid micro-off grid system has been proposed and developed. Solar and wind are two intermitted sources which are highly site specific [10]. Successful deployment of the hybrid system required solar PV resource assessment, wind resource assessment and the energy demand assessment. This paper reports on the solar PV assessment and the energy demand assessment for the three selected zones in the county. Solar PV energy is enormous than other sources of renewable energy and its systems have huge capacity to meet the ever increasing demand for energy [11], [12], [13]. Irradiance is the solar power density incident on an area from the sun [14]. The percentage of solar radiation reaching the earth's surface is greatly depended on meteorological, spatial, temporal, global and local factor which need to be accounted for when assessing its potential [15]. Kenya extends four degrees either side of the equator and as a result its locations receive a large amount of solar radiation. Assessments show that Kenya has abundant solar energy resources with a daily average solar insolation estimation of about 4-6 kWh/m$^2$, one of the best for solar energy production in Africa [16], [17]. In Machakos County, the three sites in this study lie adjacent to Machakos University which lies approximately 1.531$^0$S 37.262$^0$E and therefore their location suits them for a vast potential of solar energy generation. Areas within the equator have the sun directly above them therefore not significantly affected by the sun's declination angle. An ideal tool thus has to be sought that will accommodate all these factors. PVGIS used in estimating solar PV potential in this work is a solar-based online tool that has been used in the world to estimate PV production potentials [18]. The database in the tool was developed by use of solar radiation model *r.sun* [19], [20], [21]. This models approximates diffuse and reflected components of clear-sky and global irradiance for horizontal or slanting surfaces for a selected site within the whole of Africa, parts of Europe, America and Asia. Solar PV potential assessment was done in Nigeria using databases with monthly means of daily isolations from NASA meteorology and solar energy [22]. The analysis showed that the sites have a PV potential of over 1000 kWp/kWp. A study done in Lisbon suburb using LiDAR data and ArcGIS reported a PV potential of 11.5GWh per year at 7 MW installed capacity [23]. Other studies have been conducted elsewhere to determined PV energy production potentials by use of PVGIS and Global Horizontal Irradiance as well as *r.sun* solar radiation model [24], [25], [26], [27].

The sun and the earth are two hot bodies at different temperature levels producing radiations at different wavelengths and energy affecting the amount of solar PV energy harnessed in day time and at night. Both solar and terrestrial radiations from the two bodies are governed by radiation laws.  According to the inverse square law given by equation 1.1 [28], the intensity of radiation becomes weaker as it spreads out from the source. Solar intensity reaching the earth is weakest when the sun is furthest and highest when near,

$$I = \frac{S}{4\pi r^2} \qquad\qquad [1.1]$$

where S is the source strength and r is the distance from the source.

Wavelength and energy of emitted radiations are functions of absolute temperature. This is explained by the Wien's and Stefan-Boltzmann laws of radiation given by equation 1.2 and 1.3 [29], [30]. From Wien's law more energetic short wavelengths are emitted at high temperature whiles according to Stefan-Boltzmann law, energy radiated per unit area is directly proportional to the fourth power of absolute temperate. This explains why energy is at its optimum at midday when temperatures are highest during the day and the equinox for areas near the equator,

$$\lambda_{max} = \frac{b}{T} \qquad\qquad [1.2]$$

where b is the Wien's constant and T is the absolute temperature,

$$E = A\sigma e T^4 \qquad\qquad [1.3]$$

where A is the surface area,  is the Stefan-Boltzmann constant, e is the emissivity and T is the absolute temperature

Solar radiation reaching the earth's surface is depended on environmental conditions, period of the day, local features, ecological and biological processes, peoples' activities and inclination of the surface. In solar PV technology the variation in amount of insolation falling on a panel also differs depending on sun's position which is a factor of declination angle, latitude angle, zenith angle and azimuth angle, and sun's angle of elevation.  Latitude ($\emptyset$) is the angle that on the equatorial plane south or north of the equator. It varies from $-90^o$ and $90^o$. [31]. Declination angle($\delta$) is the angle of tilt with respect to the earth's orbit around the sun ranging from $-23.5^o$ to $23.5^o$ depending on the month and season of the year. Declination angle can be determined using equation 1.4 [31], [32]

$$\delta = 23.5 \, sin\left[\frac{(360(284+n))}{365}\right]^o \qquad\qquad [1.4]$$

where n is the day of the year starting from January 1st.

Zenith angle ($\theta_z$) is the angle between the vertical axis and the suns position $90^o$ on horizontal plane and $0^o$ at noon. This can be calculated by equation 1.5 [33],

$$cos\theta_z = Cos\delta cos\emptyset cos\omega + sin\delta sin\emptyset \qquad\qquad [1.5]$$

where $\omega$ the hour angle is determined using equation 1.6 [31], [32],

$$\omega = 15(t_s - 12) \qquad\qquad [1.6]$$

where $t_s$ is time of the solar in hours.

Solar azimuth angle $(\gamma_s)$ is the angle between the direction of due South and that of the perpendicular projection of the sun down onto horizontal line ranging from $0^o$ to $-180^o$. Azimuth angle in the northern hemisphere is south oriented whiles in the southern hemisphere is north oriented. This angle can be calculated using equation 1.7[33],

$$Cos\gamma_s = \frac{1}{COSA_Z}[\cos\delta\sin\emptyset\cos\omega - \sin\delta\cos\emptyset] \qquad\qquad [1.7]$$

Sun's angle of elevation $(\alpha)$, the angle between the horizontal plane and the sun is the complement of zenith angle $90^o$ and can be determined using equation 1.8 or 1.9[33],

$$\alpha = 90 - \theta_z \qquad\qquad [1.8]$$

$$\sin\alpha = \cos\delta\cos\emptyset\cos\omega + \sin\delta\sin\emptyset \qquad\qquad [1.9]$$

**Rationale**

Energy is vital for sustanance of any rural and urban development in the country. It is therefore necessary to ensure a balance between the energy demand and the energy supply [34], [35]. A solution thus lies in optimizing energy by use of alternative sources of energy from renewable sources [36]. Energy load demand in a region is variable with time and the standards of living of consumers. Methods of energy generation and energy systems ought to be reliable to meet the rising load demand. Energy load demand assessment is thus a necessary activity in deployment, planning and installation of energy generation and distribution systems [37], [38], [39]. Energy demand evaluation done in Kikwe Village in Tanzania reported a village daily load of 757.024 kWh with a peak load of 56 Kw and a minimum of 5 kW [37]. Rural and urban household energy demand analysis studies were done in Pakistan simulated using 2010 data as the base year by use of LEAP model. This reported a demand of 25GWh extrapolated to 170000GWh by 2036 [34]. [40] Assessed domestic energy demand of coastline of Niger Delta in Nigeria. HOMER hybrid optimization software was used to estimate the demand for determining the best PV system reporting a daily load demand estimate of 5.640 kWh. By 2015 installed capacity of Tanzania was 1129 MW which was not enough to serve both rural and urban areas due to high consumption rate [41], [42]. Sparse demography is one of the factors that hinder national grid development in rural and semi urban areas making it costly to set up [43], [44], [44]. This makes renewable sources like wind and solar promising in creation of energy access to consumers [46], [17].

**MATERIALS AND METHODS**

Successful design and development of a suitable renewable energy system requires investigation and analysis of the critical parameters that determine the amount of solar radiation reaching the earth's surface. In solar PV assessment factors such as latitude and longitude of the selected site, solar declination angle, PV module, and orientation and inclination need to be investigated to enable optimum solar harvest from the available insolation.

**Solar PV Estimation using PVGIS**

A typical hardware setup to estimate PV potential for energy production in a site entails data logger, solar PV modules and sensors. The online simulation software was used to determine the various parameters of the solar PV system at Machakos County. Depending on the input parameters it estimates the daily and monthly irradiance, yearly PV energy yields, yearly solar in-plane irradiance and the total system losses [27]. The simulation was done through the following steps

Step 1: Start the PVGIS online simulation

Step 2: Choose the data base- PVGIS-CMSAF.

Step 2: Enter the latitude and longitude of the zones A, B and C.

Step 3: Choose the PV technology- Crystalline Silicon

Step 4: Enter the systems installed capacity – 1kWp

Step 5: Enter the system loss allowance- 5%

Step 6: Choose the azimuth, the orientation angles and tracking option $10^o$ and $-180^o$ respectively.

Step 7: Run the simulation. A report is produced containing all the required solar PV parameters at a specific site.

The three complements of solar energy conversion technology obtained from the simulation include the global horizontal irradiance (GHI) measured using unshaded pyranometer, diffuse horizontal irradiance (DHI) measured using shaded pyranometer and direct normal irradiance (DNI) measured using pyrheliometer [47]. DNI is the available radiation at about 5o view on a surface normal to the sun, DHI is the scattered radiation from the sky while GHI is the sum of DNI and DHI components given by equation 2.0 [48],

$$GHI = DNI \; \cos(\theta_z) + DHI \qquad\qquad [2.0]$$

where $\theta_z$ is the zenith angle.

Solar irradiance was also measured by use of MS-602 model pyramometer mounted at 20 m above the ground level to avoid shading effects from building and trees. The sensor was connected to a data logger set to capture the irradiance values at a frequency of 1Hz. figure 1 and 2 show the plates of the solar radiation sensor and the data logging system used.

Plate 1: MS-602 Pyranometer used to measure GHI at the site



Plate 2: Data logging system

**Energy load demand estimation**

Primary data was collected by use of a suitable questionnaire designed to capture all parameters of energy consumption and the information on household's status. A survey was undertaken to assess the electrical energy load demand in the villages contained in each of the three zones A, B and C which contains 300 households on average. A sample of 100 households was used to investigate the load pattern in each zone and projection of the demand for the whole zone. Interviews were conducted for 20 days in rural homes, schools, shopping centers and the sampled households per zone to make a good judgement of the electrical appliance used, installed source of energy, household size, monthly income and the time of used of each electrical appliance per day. The common household's loads in the three zones were phones, bulbs, TV sets, radio, heater, iron box, hoofers, hair drier and blenders. A few households contained appliances like fridge, oven and cookers which consume slightly higher energy.

Daily totals, averages load requirements per zone were determined by use of equations 2.1 and 2.2 respectively,

$$E_{Total} = \sum_i^N p^k t \qquad\qquad [2.1]$$

where E is the energy, P is the power rating of the appliance, k represents an appliance, t is the time of use and N is the number of appliances,

$$E_A = \frac{1}{N_H} \sum_i^N p^k t \qquad\qquad [2.2]$$

where $E_A$ is the daily average value per zone, $N_H$ is the total number of households per zone. Energy load demand and monthly income profiles were plotted which gave a good pattern of the energy consumption and economic status of the inhabitants in zones A, B and C.

**RESULTS AND DISCUSSION**

**Solar PV**

Solar PV assessment results were analyzed and profiles generated using the PVGIS software. Figure 1(a), 1(b), 1(c) show the hourly range of global, diffuse, direct clear sky irradiance in Machakos sites compared monthly. Table 1 and 2 show the distribution of GHI, DHI, DNI at real sky and clear sky both at fixed plane and tracking option. Comparatively irradiance is higher when tracking option is used since the sun rays are always normal to the plane of the PV module.

Table 1: Daily average Peak Values of GHI, DHI, DNI and CSI at Fixed Plane

| Month | GHI(W/m$^2$) | DNI(W/m$^2$) | DHI(W/m$^2$) | CSI (W/m$^2$) |
|---|---|---|---|---|
| January | 898 | 682 | 215 | 1040 |
| February | 969 | 749 | 219 | 1100 |
| March | 965 | 719 | 244 | 1140 |
| April | 906 | 626 | 279 | 1130 |
| May | 741 | 434 | 306 | 1090 |
| June | 638 | 326 | 311 | 1070 |
| July | 619 | 310 | 308 | 1080 |
| August | 649 | 325 | 324 | 1120 |
| September | 853 | 596 | 256 | 1120 |
| October | 882 | 609 | 273 | 1080 |
| November | 817 | 549 | 267 | 1030 |
| December | 812 | 575 | 245 | 995 |

Table 2: Daily Average Peak Values of GHI, DHI, DNI and CSI at PV tracking

| Month | GHI(W/m$^2$) | DNI(W/m$^2$) | DHI(W/m$^2$) | CSI (W/m$^2$) |
|---|---|---|---|---|
| January | 1030 | 800 | 222 | 1190 |

| | | | | |
|---|---|---|---|---|
| **February** | 1030 | 807 | 223 | 1180 |
| **March** | 973 | 723 | 250 | 1150 |
| **April** | 908 | 631 | 274 | 1140 |
| **May** | 770 | 464 | 301 | 1120 |
| **June** | 660 | 347 | 307 | 1120 |
| **July** | 621 | 318 | 297 | 1120 |
| **August** | 650 | 326 | 321 | 1130 |
| **September** | 867 | 611 | 255 | 1130 |
| **October** | 915 | 628 | 285 | 1140 |
| **November** | 918 | 663 | 245 | 1160 |
| **December** | 946 | 681 | 258 | 1170 |

Figure 1(a) and (b), 2(a) and (b), and 3(a) and (b) show the daily average irradiance profiles at fixed plane and tracking option in the March, October and June when maximum and minimum PV output is expected.
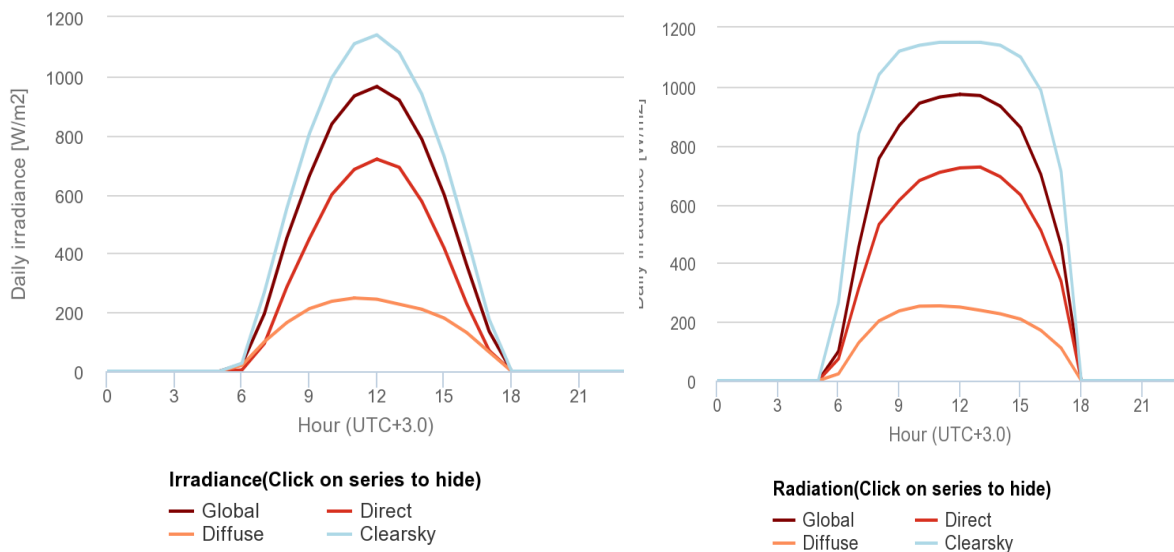
Figure 1(a) and 1(b): Fixed plane and tracking daily average irradiance in March
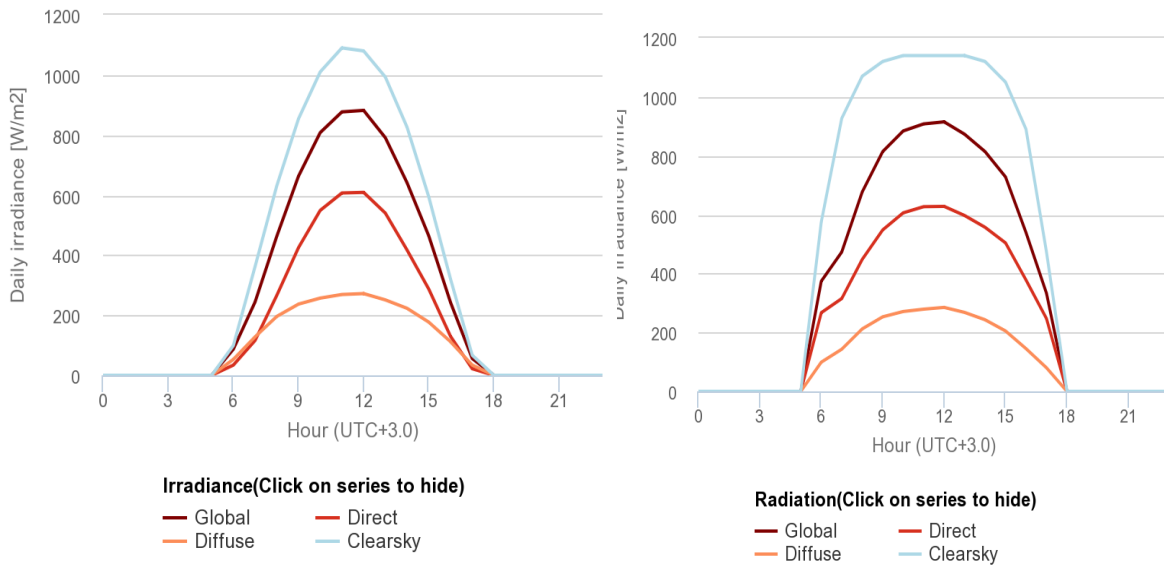


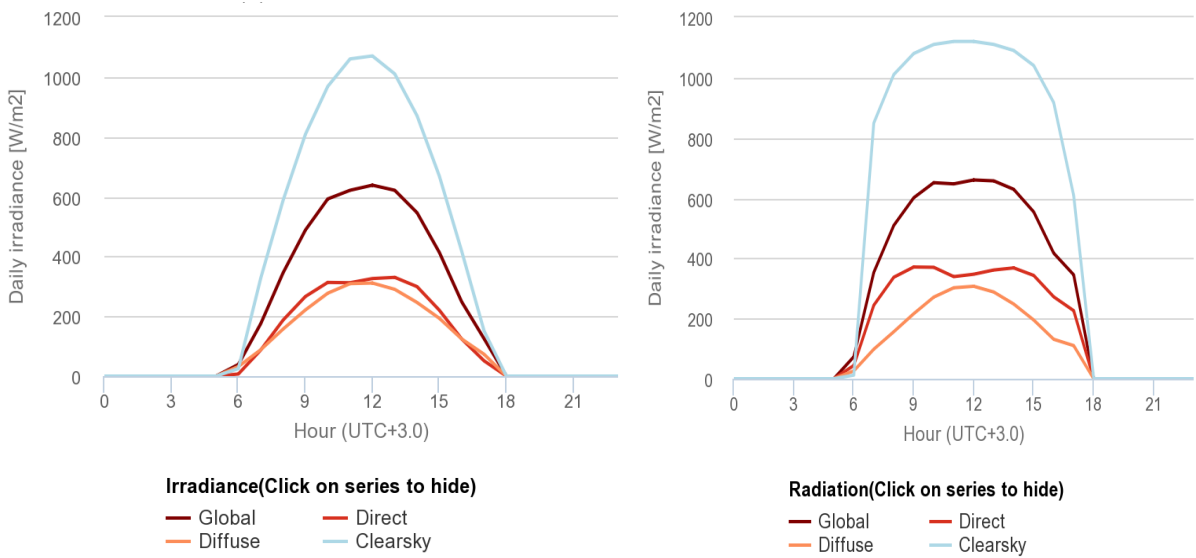Figure 2(a) and (b): Fixed plane and tracking daily average irradiance in October



Figure 3(a) and (b): Fixed plane and tracking daily average irradiance in June

In the month of January to March and September to December, the peak global irradiance received is between 900 - 1000 $W/m^2$ and 850 - 900 $W/m^2$ respectively while in June and July 638-619 $W/m^2$ is received at fixed plane. Machakos region being near the equator experiences the four season's summer and Winter solstice and the equinox (vernal and autumnal). Daily solar intensity is maximum during the equinox in March and September when the earth rotates with the equator in line with the suns central plane.

Data analysis of measured solar irradiance values was done for comparison with the PVGIS simulated values. The data was tabulated on hourly and daily basis with the peak and average irradiance values. Table 3 shows the experimental average and peak GHI values in the month of March. Hourly and daily solar irradiance profiles were plotted to show the solar insolation pattern in Machakos. Figure 4 and 5 show the hourly and daily solar irradiance profiles.

Table 3: Hourly mean and peak solar irradiance

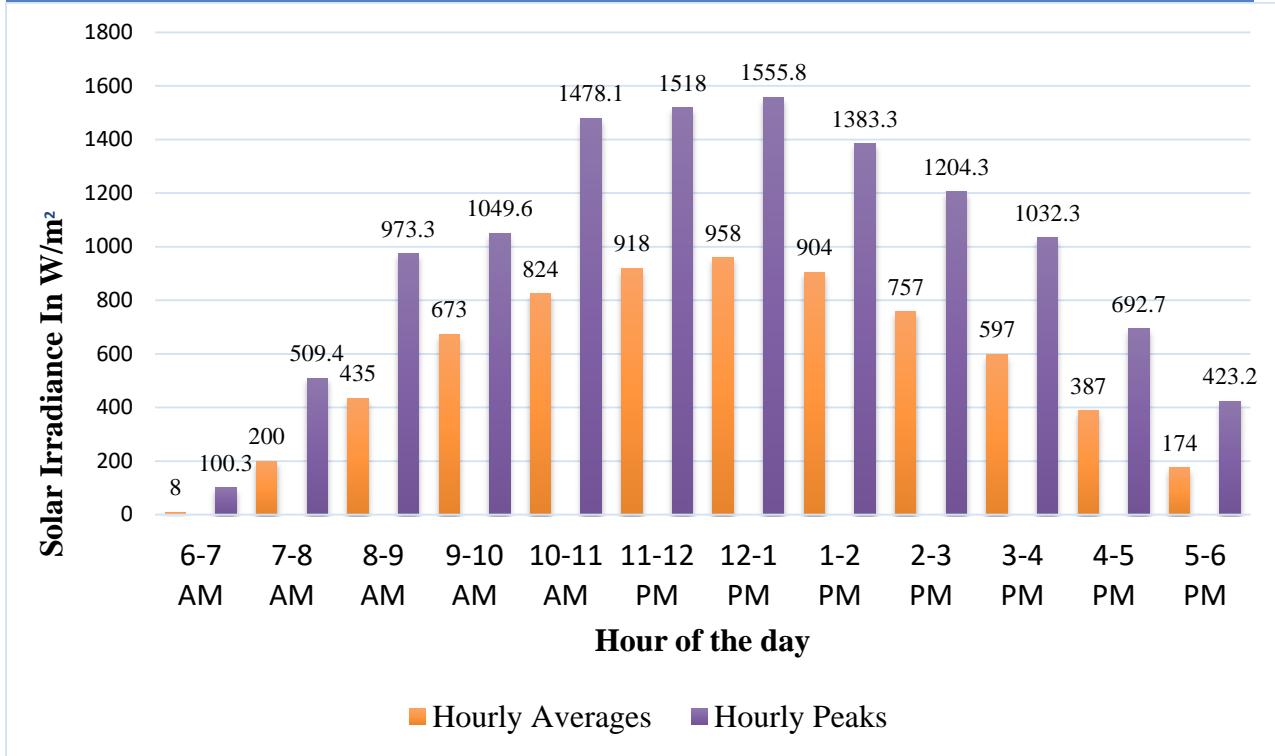| Hour | Average GHI (W/m$^2$) | Peak Average GHI ( W/m$^2$) | Peak GHI ( W/m$^2$) |
|---|---|---|---|
| 6-7 AM | 8 | 58 | 100.3 |
| 7-8 AM | 200 | 384 | 509.4 |
| 8-9 AM | 435 | 659 | 973.3 |
| 9-10 AM | 673 | 898 | 1049.6 |
| 10-11 AM | 824 | 1121 | 1478.1 |
| 11-12 PM | 918 | 1208 | 1518 |
| 12-1 PM | 958 | 1228 | 1555.8 |
| 1-2 PM | 904 | 1140 | 1383.3 |
| 2-3 PM | 757 | 1035 | 1204.3 |
| 3-4 PM | 597 | 816 | 1032.3 |
| 4-5 PM | 387 | 578 | 692.7 |
| 5-6 PM | 174 | 306 | 423.2 |

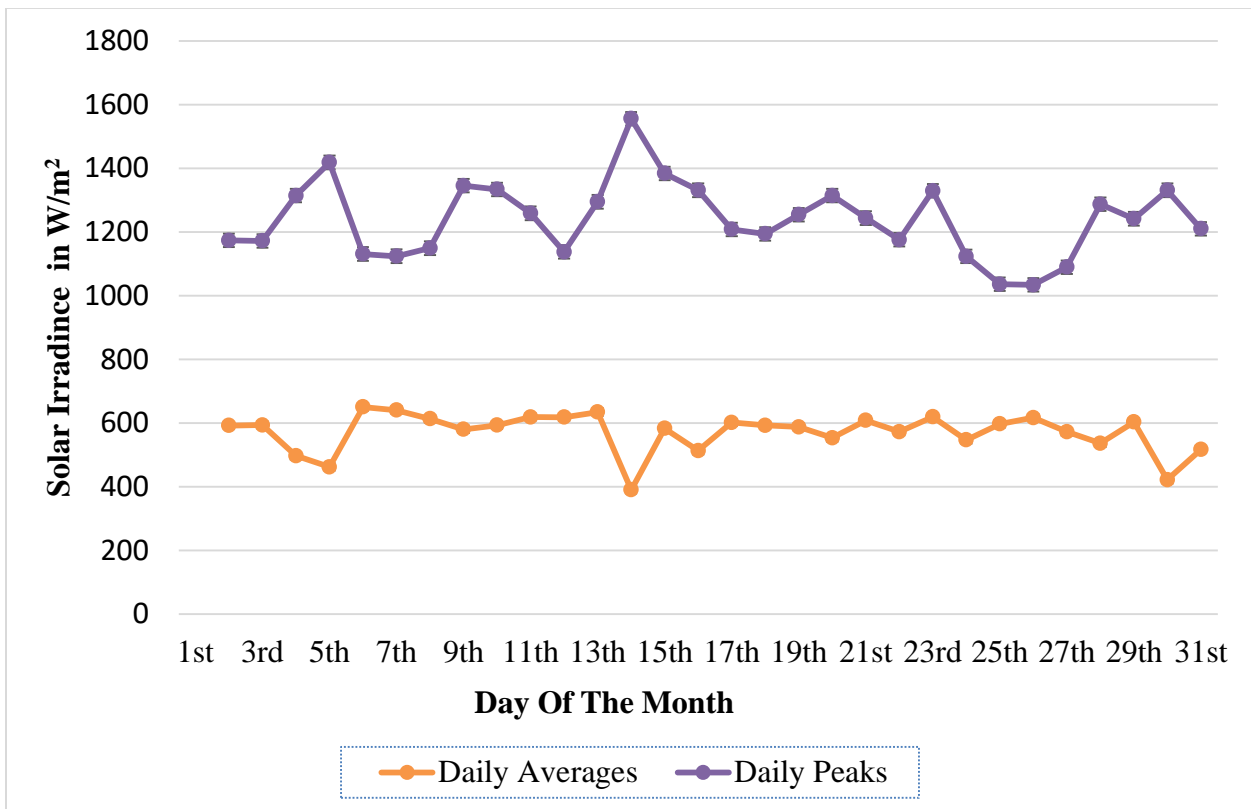Figure 4: Hourly mean and peak solar irradiance



Figure 5: Daily mean and peak solar irradiance

Machakos receives solar insolation up to a maximum peak of 1555.8 W/m$^2$ with peak average of 1228 W/m$^2$ at noon during clear sky. Shading effect due to clouds reduces the hourly average peak to 958 W/m$^2$ which is still high at suitable for optimum solar PV energy harvest. Solar radiation was analysed on daily basis for 31 day. Peak solar insolation in Machakos lies between 1000 W/m$^2$ and 1600 W/m$^2$ and 400 to 600 W/m$^2$ as a result of cloud shading effect. This shows the huge daily and monthly solar PV potential Machakos County has.

Figure 6 shows the path of the sun and the solar window for Machakos county zones form June 21$^{st}$ to December 21$^{st}$. The sun shines directly above the equatorial zones with a solar window of 12 hours between 6 am and 6 pm. In this zone the sun's declination is $0^o$ and the radiation covers the shortest distance to reach the earth and from the laws of radiation the intensity of radiation is maximum, the earth surface if more hot than other seasons. Therefore, during the equinox the earth receives higher insolation which gives maximum solar PV energy at midday.
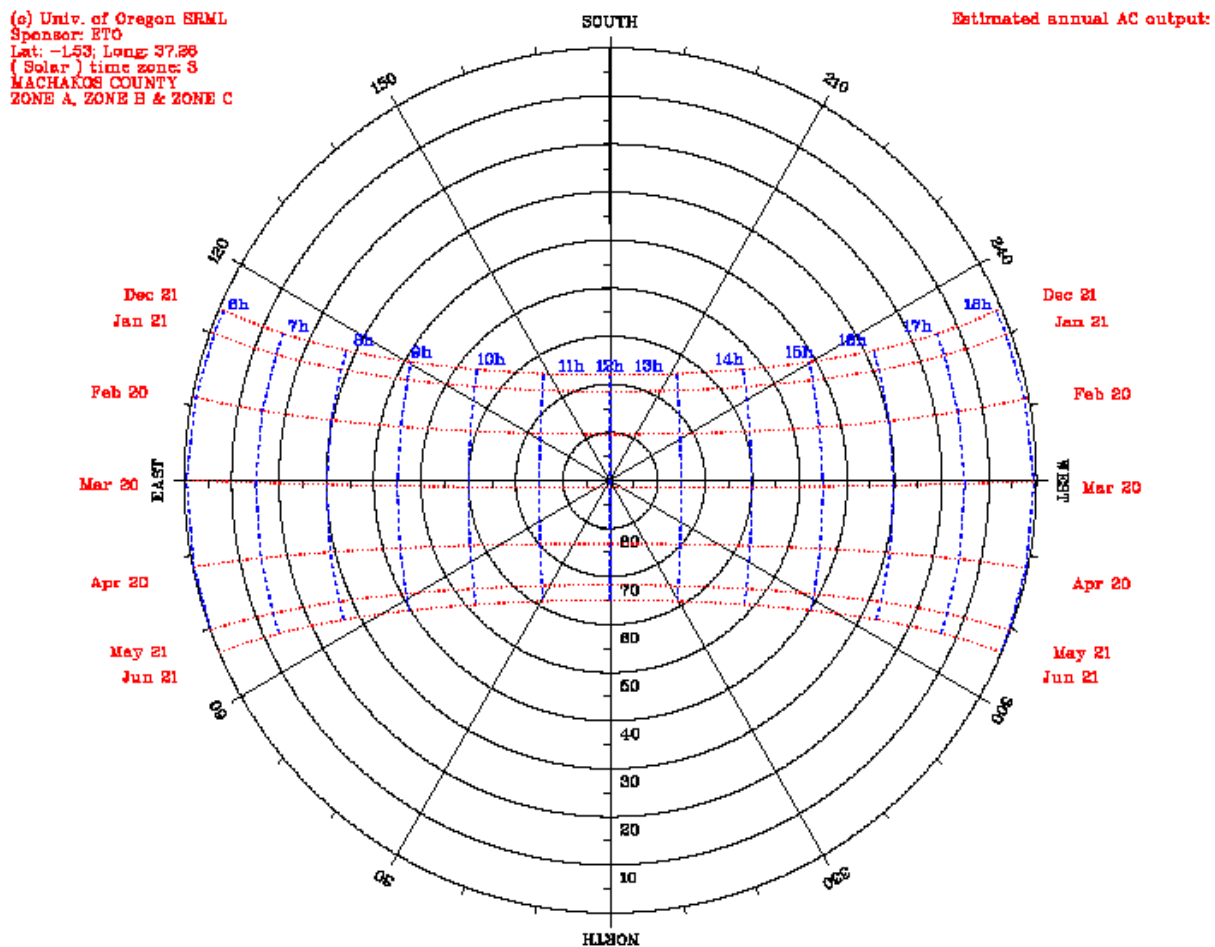


Figure 6: Sun path diagram for Machakos zone.

Due to its revolution in an elliptical orbit the earth experiences four seasons. During the Winter solstice the sun is at its shortest distance from the earth approximately $1.47 \times 10^{11}$m. The sun shine is at a declination angle of $-23.5^o$ directly on the tropic of Capricorn in the southern

hemisphere maximum in December 21st. This increases the solar intensity for all the regions in the southern hemisphere like Machakos County. In June and July, the earth experiences the summer solstice and at the furthest distance from the sun, approximately $1.52 \times 10^{11}$m. The sun is high up shining directly at the tropic of cancer at a maximum declination angle of $23.5^{o}$. Solar intensity is high at northern hemisphere and low in southern hemisphere. This makes Machakos zones register low daily irradiance. Solar irradiance compared between azimuth angle of $10^{o}$ simulated and analyzed. Figure 7 show the simulated monthly output values of irradiance at fixed angle. The simulated annual in plane irradiation at Machakos was 2130 kWh/m$^{2}$. This tilt makes the sun more direct to the panel than when in horizontal orientation
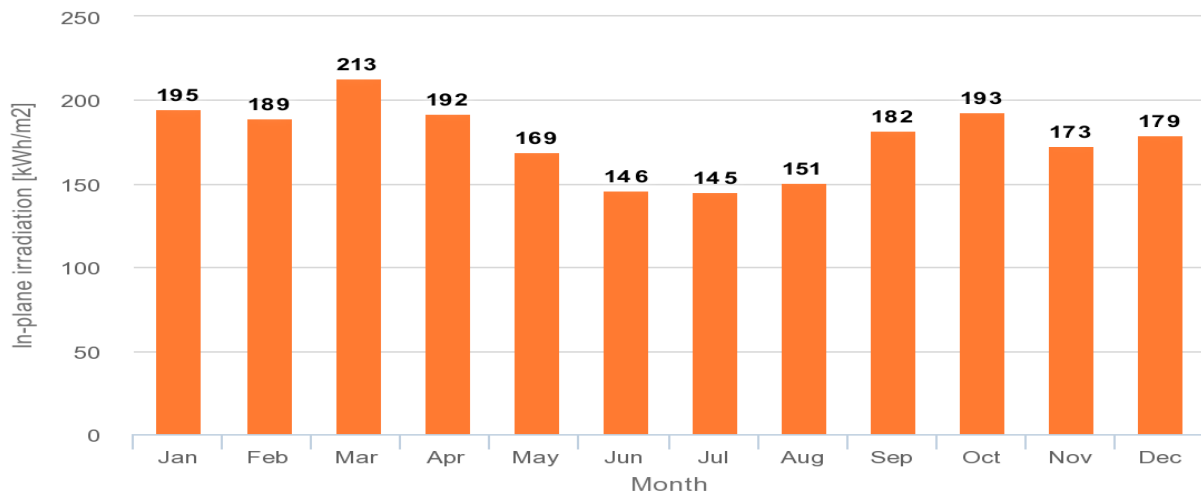


Figure 7: Monthly in-plane irradiance at fixed-angle solar PV system

The first and the last four months of the year have higher during the equinox and the winter solstice. The average monthly peak values are 213 kWh/m$^{2}$ and 193 kWh/m$^{2}$ in March and October. Yearly PV energy production was also investigated at $10^{o}$ of panel tilt. Figure 8 show monthly energy output profile. Machakos region has a potential of producing an annual solar PV energy of 1740 kWh. The months when the sun is closest to the equator have a higher energy potential on average compared to months summer solstice months when the sun is furthest from the equator. The month of March has the maximum average potential of 170 kWh while June and July have the minimum potential of 123 kWh and 122 kWh respectively.
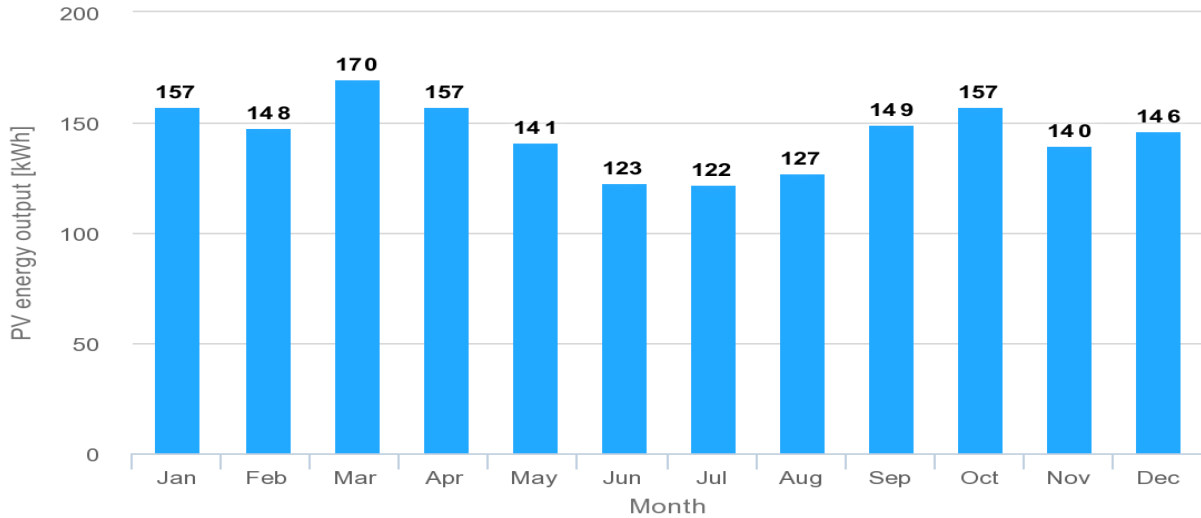
Figure 8: Monthly average energy production at fixed angle solar PV system

**Load Demand**

Daily energy load estimates, installed PV capacity estimates, PV module estimates and the battery storage capacity estimates per zone were tabulated as shown. Table 4 shows the loads estimates in zone A, zone B, and zone C.

Table 4: Daily Energy load demand estimates

|  | Zone A-4.3 sq.km | Zone B-4.2 sq.km | Zone C-4.9 sq.km |
|---|---|---|---|
| Whole Zone | 782.7 kWh | 841.2 kWh | 620.02 kWh |
| Average per household | 2.429 kWh | 2.26 kWh | 2.347 kWh |
| Max household | 9.09 kWh | 5.37 kWh | 7.844 kWh |
| Min household | 0.24 kWh | 0.052 kWh | 0.135 kWh |

Zone B is comprised of four villages and therefore has the highest daily load of 841.2 kWh while C has the least. On average Zone A consumes more energy per house hold compared to the other two zones. Peak household consumption was determined as 9.09 kWh in zone A and a minimum household energy consumption of 0.052 kWh. Table 5 shows the calculated installed capacities up scaled by a factor of 30% to cater for the system losses.

Table 5: PV System capacity Estimates

|  | Zone A | Zone B | Zone C |
|---|---|---|---|
| Whole Zone | 213.45 kW$_P$ | 229.4 kW$_p$ | 169.08 kW$_p$ |

| | | | |
|---|---|---|---|
| Average per household | 0.6624 KW$_p$ | 0.6163 kW$_P$ | 0.64 kW$_P$ |
| Max House Hold | 2.479 KW$_p$ | 1.4638 kW$_P$ | 2.139 kW$_P$ |
| Min House Hold | 0.0654 kW$_P$ | 0.014 kW$_P$ | 0.037 kW$_P$ |

The energy peaks were calculated using equation and the PV yearly energy production of 1740 kWh per kWp simulated using the PVGIS. Table 6 shows the estimated solar Modules based on the upscale solar peaks in the three zones. Canadian solar panel with an output power of 350 W was used in the estimations

Table 6: PV Module Estimate based on simulated annual PV energy production

| | **Zone A** | **Zone B** | **Zone C** |
|---|---|---|---|
| Whole Zone | 610 Panels | 655 Panels | 484 Panels |
| Average per household | 2 Panels | 2 Panels | 2 Panels |
| Max household | 8 Panels | 5 Panels | 7 Panels |
| Min household | 1 Panel | 1 Panel | 1 Panel |

In comparison zone B requires more solar panels to meet the estimated load demand. On average 2 panels would meet the demands in most of the households with a minimum and maximum of 1 and 8 panels in some households respectively. Number of module estimation was also done based on the month with the minimum solar irradiance if 145 kWh/m2 and 4.6773 peak hours per day. Table 7 shows the estimated PV modules in the three zones based on peak hours.

Table 7: PV module estimate based on the minimum month solar irradiance

| | *Zone A* | *Zone B* | *Zone C* |
|---|---|---|---|
| Whole Zone | 638 Panels | 686 Panels | 505 Panels |
| Average per household | 3 Panels | 2 Panels | 2 Panels |
| Max household | 8 Panels | 5 Panels | 7 Panels |
| Min household | 2 Panel | 1 Panel | 1 Panel |

The number of PV modules requires is comparatively similar on average and for the households with maximum and minimum energy consumption levels. Based on the month of June and July, each of the three zones would require slightly a higher number of panels for solar energy harvest

to meet the same load demand. The minimum month approach is therefore more suitable in PV system sizing since the PV system ought to operate normally throughout the year with all solar insolation variations factored in.

Energy storage battery capacities were also determined using the load demands in table 4. Lithium ion battery was considered due to its higher depth of discharge of approximately 80% compared to the lead acid accumulators which of about 50%. Table 8 shows the estimated battery capacities for the three zones.

Table 8: Battery Capacity Estimate based on the energy demands

|  | Zone A | Zone B | Zone C |
|---|---|---|---|
| Whole Zone | 81531.25 AH | 87625 AH | 64585.42 AH |
| Average per household | 506.04 AH | 470.84 AH | 488.96 AH |
| Max household | 1893.75 AH | 1118.76 AH | 1634.16 AH |
| Min household | 100 AH | 21.68 AH | 56.24 AH |

A comparative daily energy load and monthly income profiles were plotted to show rate of energy use at different hours and the economic status of the consumers in each zone as shown in figure 9. In three zones the energy use pattern is similar, higher from 1700 hours to 2200 hours and lowest from mid night to 0400 hours.
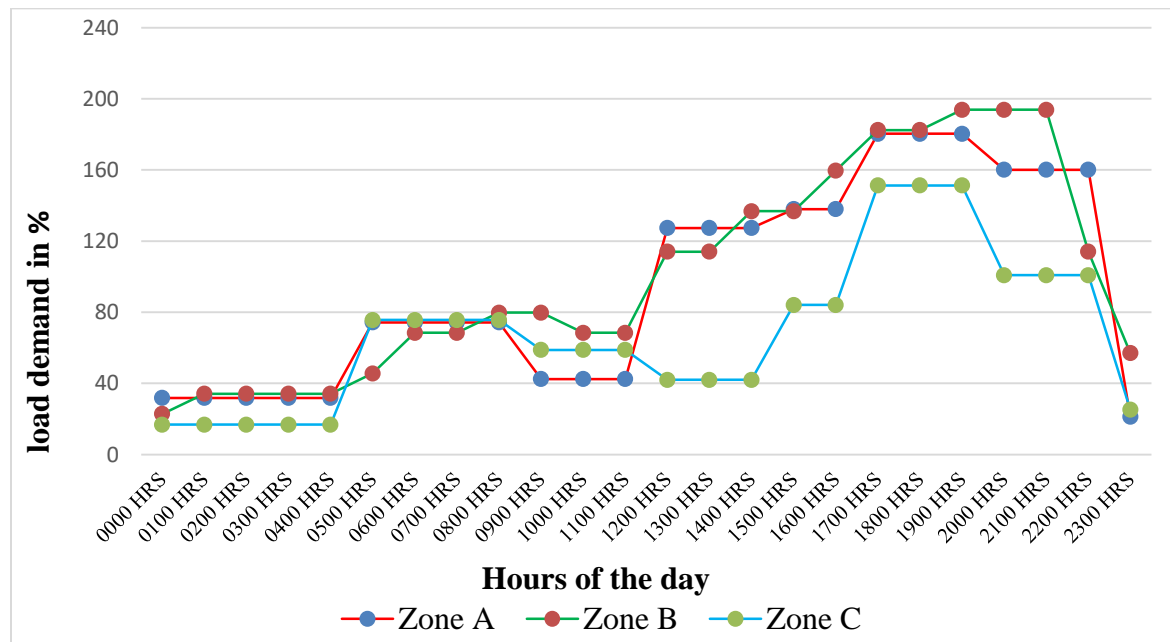


Figure 9: Daily load energy demand profile

High energy demand between 5 pm and 10 pm can be attributed to the fact that most of the household members are back home from their daily activities and make use of energy more than other times for the various domestic needs like lighting, entertainment and cooking. Demand is low from mid night since most of the people are asleep and therefore less energy is used probably for security lighting. From 5 am energy is used as people prepare to leave for work. This profile shows that there is no zero energy demand in the selected sites. This justifies the need for a constant electricity supply in the rural areas of Machakos County.

Economic status analysis was also done and data tabulated and analyzed as shown in table 8 and figure 10 respectively. Most of the occupants in the rural areas are low income earners with an average of ksh 15000 per month. This explains why most people in the zones lack expensive appliances like machines that consume huge amounts of power. Cost of electricity comprises of acquisition cost, operating cost, maintenance cost and replacement costs which are far beyond the financial ability of most people. A cheap renewable hybrid power system was therefore more suitable for energy generation in small scales for the rural zones

Table 8: Households monthly income per zone

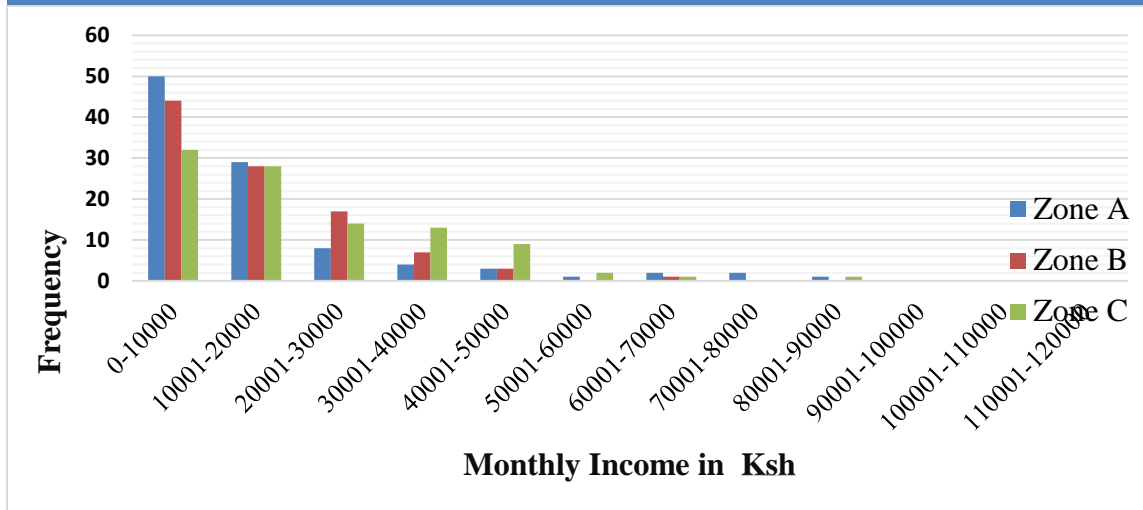| Household Monthly Income in Ksh | Zone A | Zone B | Zone C |
| --- | --- | --- | --- |
| 0-10000 | 50 | 44 | 32 |
| 10001-20000 | 29 | 28 | 28 |
| 20001-30000 | 8 | 17 | 14 |
| 30001-40000 | 4 | 7 | 13 |
| 40001-50000 | 3 | 3 | 9 |
| 50001-60000 | 1 | 0 | 2 |
| 60001-70000 | 2 | 1 | 1 |
| 70001-80000 | 2 | 0 | 0 |
| 80001-90000 | 1 | 0 | 1 |
| 90001-100000 | 0 | 0 | 0 |
| 100001-110000 | 0 | 0 | 0 |
| 110001-120000 | 0 | 0 | 0 |

Figure 10: Monthly income profile

## CONCLUSION

The solar simulation and experimental solar assessment results show huge potential of solar energy in Machakos County suitable for small scale hybrid system installation for PV energy production. Machakos County has a yearly average solar irradiance of 2130 kWh/m$^2$ with an average and peak hourly GHI of and 1556 W/m$^2$ respectively. Simulated PV energy production from these radiation levels gives a yearly average PV energy potential of over 1740 kWh at 1 kW peak installed capacity. Energy utilization assessment show that Machakos county rural areas consume less energy comparatively due to the type and number of appliances available. Much energy is used in the evening and at night when people are back home from job. Zone A, B and C consume 782.7 kWh, 841.2 kWh, and 620.02 kWh per day with a household average consumption of 2.345 kWh per day. The available solar insolation was used as reference in estimating the installed capacities and PV system size suitable for rural electrification in Machakos.

## RECOMMENDATION

With the huge solar PV potential, Machakos County has the capacity to support a solar photovoltaic systems for off-grid electrification.

## REFERENCES

[1] Omer, A. M. (2008). Energy, environment and sustainable development. *Journal of Renewable and Sustainable Energy Reviews.***12**, 2265. (doi:10.1016/j.rser.2007.05.001)

[2] Mukulo, B., Ngaruiya, J., and Kamau, J. (2014). Determination of wind energy potential in

The Mwingi-Kitui plateau of Kenya, *Renewable Energy* **63**, 18-22.

[3] Kenya Climate Innovation Centre (). Kenya Solar PV Market and Assessment Report.

[4] Wakui, T., and Yokoyama, R., (2013). Wind Speed Sensor less Performance Monitoring Based on Operating Behavior for Stand-Alone Vertical Axis Wind Turbine. *Renewable Energy* **53**,49-59.

[5] AslamBhutta, M. M., Hayat, N., Farooq, A. U., Ali, Z., Jamil, S. R., and Hussain, Z. (2012).Vertical axis wind turbine-a review of various configurations and design techniques. *Journal of Renewable and Sustainable Energy Reviews*.**16**, 1926–1939.

[6] Granqvist, C. G. (2007). Transparent conductors as solar energy materials: a panoramic review. *Solar Energy Materials. Solar Cells* **91**, 1529. (doi:10.1016/j.solmat.2007.04.031)

[7] Granqvist, C. G. (2003). Solar energy materials. *Advanced Materials.* **15**, 1789–1803. (doi:10.1002/adma.200300378)

[8] Granqvist, C. G. (1990) Window coatings for the future. *Thin Solid Films*. **193**–**194**, 730.

[9] Skretas, S. B. and Papadopoulos, D. P. (2009). Efficient design and simulation of an expandable hybrid (wind photovoltaic) power system with MPPT and inverter input voltage regulation features in compliance with electric grid requirements. *Electric Power Systems Research* **79**(9), 1271-1285

[10] *Abbess, J. (2009).*Wind Energy Variability and Intermittency in the UK .*Claverton-energy. com.* Archived *from the original in 2011.*

*[11] Tarai, R. K. and Kale, P. (2016). Development of Rasterized mapping PVGIS for assessment of solar PV energy potential of Odisha. International Journal of Renewable Energy Research. 6 (1).*

*[12]* International Funds Corporation (IFC). (2012). Utility scale solar power plants: A guide for developers and investors, South Asia Department, New Delhi, India

[13] Mulaudzi, S. K. (2016). An Assessment of the Potential of Solar Photovoltaic (PV) Application in South Africa.

[14] Syafawati, A. N., Daut, I., Irwanto, M., Farhana, Z., Razliana, N., Arizadayana, Z., and Shema, S. S.(2012) Potential of solar energy harvesting in Ulu Pauh, Perlis, Malaysia using solar radiation – Analysis studies, 2011 2nd International Conference on Advances in Energy Engineering (ICAEE 2011), Energy Procedia **14**,1503 – 1508

*[15] Redweik, P., Catita, C., and Brito, M. (2013). Solar Energy Potential on Roofs and facades in an urban land scape. Solar Energy.97, 332-341.*

*[16] Theuri, D. (2008). Solar and Wind Energy Resource Assessment Report. SWERA National Team. Nairobi.*

[17] Tigabu, A. (2016). A dest assessment on the overview of current solar and wind energy projects in Kenya. IREK report No: 1.

*[18]* Hulda, T., Mullerb, R. and Gambardella, A. (2012). A new solar radiation database for estimating PV performance in Europe and Africa. **86** (6), 1803–1815.

*[19]* Hofierka, J. and Suri, M. (2002). The solar radiation model for Open source GIS: implementation and applications. In*: Proceedings of the Open source GIS – GRASS Users Conference*. Trento, Italy, 11–13 September

[20] Suri, M., Huld, T. A., Dunlop, E. D., and Ossenbrink, H. A. (2007). Potential of solar electricity generation in the European Union member states and candidate countries. *Solar Energy* **81**, 1295-1305

[21] Suri, M., Dunlop, E. D., Huld, T. A., (2005). PV-GIS: A web based solarradiation database for the calculation of PV potential in Europe. *International Journal of Sustainable Energy 24* (2), 55–67.

*[22]* Njoku, H. O. (2014). Solar Photovoltaic Potential in Nigeria. *Journal of Energy Engineering,* 1-7.

[23] Brito, M.C., Gomes, N., Santos, T. and Tenedorio, J. A. (2012) Photovoltaic potential in a Lisbon suburb using LiDAR data. *Solar Energy.* 283-288.

[24] Gómez-Gil, F. J., Wang, X. and Barnett, A. (2012). Analysis and Prediction of Energy Production in Concentrating Photovoltaic (CPV) Installations. **5** (3), 770-789.

[25] Hofierka, J. and Kanuk, J. (2009). Assessment of photovoltaic potential in urban areas using open-source solar radiation tools. **34** (10), 2206–2214.

[26] Suri, M., Huld, T. A., Dunlop, E.D., Albuisson, M. and Wald, L. (2006). Online Data and Tools for Estimation of Solar Electricity in Africa: The Pvgis Approach. 1-4.

[27] Dondariya, C., Porwal, D., Awasthi, A., Shukla, A.K., Sudhakar, K., Murali Manohar, S.R., and Bhimte, A. (2018). Performance Simulation of Grid-Connected Rooftop Solar PV System for Small Households: Case Study of Ujjain, India. *Energy Reports.* **4,** 546-553

[28] Kezerashvili, R. Y. (2009). Light and Electromagnetic Waves Teaching in Engineering Education. *International Journal of Electrical Engineering Education*. 343-353.

[29] Johnson, C. (2012. Mathematical physics of blackbody radiation. Icarus eBooks.

[30] Marr, J. M. and Wilkin, F. P. (2012). A better presentation of planks radiation law. *American Journal of Physics* **80**, 399.

[31] Cengiz, M. S. and Mamis, M. S (2015). A research on determining the panel inclination angle in terms if the place and seasons. *Journal of Multidisciplinary Engineering Science and Technology*. **2**(8), 2172-2177.

[32] Karafil, A., Ozbay, H., Kesler, M. and Parmaksiz, H. (2015). Calculation of optimum fixed angle of PV panels depending on solar angles and comparison of the results with experimental study conducted in summer in Bilecik, Turkey. 9th International Conference on Electrical and Electronics Engineering (ELECO), at Bursa, 971-976.

[33] Sproul, A. B. (2007). Derivation of Solar Geometric Relationships using Vector Analysis. *Renewable Energy*. **32**, 1187-1205.

[34] Urooj, R., Shabbir, R., Taneez, M. and Ahmad, S. S. (2013). Rural and Urban Household Demand Analysis for Electricity in Pakistan. International Journal of Emerging Trends in Engineering and Development. **3**(6), 185-191.

[35] USAID Kenya and East Africa. (2016). Development of Kenya Power Sector 2015-2020. Kenya Power Sector Report.

[36] Government of Kenya. (2015). Situational Analysis of energy industry, policy and strategy for Kenya. Institutive of economic affairs (IEA).

[37] Mwakitakima, I. J. (2015). Electricity Demand Evaluation for Rural Electrification. *IJERT*. 4(6), 1025-1028.

[38] Lin, B. Q. and Quising, P. F. (2003). Electricity demand in the People's Republic of China investment requirement and environmental impact, Asian Development Bank, **37.**

[39] Seppala, A. (1996). Load Research and Load Estimation in Electricity Distribution. Technical Research Centre of Finland.

[40] Diemuodeke, E. O., Addo, A., Dabipi-Kalio, I., Oko, C.O.C., and Mulugetta, Y. (2017). Domestic Energy Demand Assessment of Coastline Rural Communities with Solar Electrification. *Energy and Policy Research*. **4**(1), 1-9.

[41] Ondraczek, J. (2011). The Sun Rises in the East (of Africa): The Development and Status of the Solar Energy Markets in Kenya and Tanzania. 2nd Symposium Small PV Applications, Ulm.

[42] Msyani, M. (2013). Current status of energy sector in Tanzania: Executive exchange of developing an ancillary service market, from http://www.google.com, Feb-March.

[43] Kassenga, G. (2008). The status and constraints of solar photovoltaic energy development in Tanzania‖. Energy Sources, Part B, **3 (**4), 420-432.

[44] Kabaka, K. T., and Gwang'ombe, F (2007). Challenges in small hydropower development in Tanzania: rural electrification perspective. International Conference on Small Hydropower–Hydro. Sri Lanka.

[45] Government of Kenya. (2018). Updated Least Cost Power Development Plan. Study Period 2017-2037.Nairobi.

[46] Government of Kenya (2016). Sustainable Energy for All Kenya Investment Prospectus. Ministry of Energy and Petroleum Report. Nairobi.

[47] Stoffel, T., Renne, D., Myers, D., Wilcox, S. Sengupta, M. George, R. and Turchi, C. (2010). Concentrating Solar Power. Best Practices Handbook for the collection and Use of Solar Resource Data. Golden, Colorado. National Renewable Energy Laboratory. 146

[48] Zell, E., Gasim, S., Wilcox, S., Katamoura, S., Stoffel, T., Shibli, H., Engel-Cox, J. and Al Subie, M. (2015). Assessment of Solar Radiation in Saudi Arabia. *Solar Energy*. 119, 422-43